

## Accepted Manuscript

A new fluorene-based Schiff-base as fluorescent chemosensor for selective detection of Cr<sup>3+</sup> and Al<sup>3+</sup>

Mahmood Tajbakhsh, Gholam Babaei Chalmardi, Ahmadreza Bekhradnia, Rahman Hosseinzadeh, Nahid Hasani, Mohammadreza Azizi Amiri



PII: S1386-1425(17)30636-4

DOI: doi: [10.1016/j.saa.2017.08.007](https://doi.org/10.1016/j.saa.2017.08.007)

Reference: SAA 15364

To appear in: *Spectrochimica Acta Part A: Molecular and Biomolecular Spectroscopy*

Received date: 4 May 2017

Revised date: 6 July 2017

Accepted date: 1 August 2017

Please cite this article as: Mahmood Tajbakhsh, Gholam Babaei Chalmardi, Ahmadreza Bekhradnia, Rahman Hosseinzadeh, Nahid Hasani, Mohammadreza Azizi Amiri, A new fluorene-based Schiff-base as fluorescent chemosensor for selective detection of Cr<sup>3+</sup> and Al<sup>3+</sup>, *Spectrochimica Acta Part A: Molecular and Biomolecular Spectroscopy* (2017), doi: [10.1016/j.saa.2017.08.007](https://doi.org/10.1016/j.saa.2017.08.007)

This is a PDF file of an unedited manuscript that has been accepted for publication. As a service to our customers we are providing this early version of the manuscript. The manuscript will undergo copyediting, typesetting, and review of the resulting proof before it is published in its final form. Please note that during the production process errors may be discovered which could affect the content, and all legal disclaimers that apply to the journal pertain.

# A new fluorene-based Schiff-base as fluorescent chemosensor for selective detection of $\text{Cr}^{3+}$ and $\text{Al}^{3+}$

Mahmood Tajbakhsh<sup>a\*</sup>, Gholam Babaei Chalmardi<sup>a</sup>, Ahmadreza Bekhradnia<sup>b</sup>, Rahman Hosseinzadeh<sup>a</sup>, Nahid Hasani<sup>a</sup>, Mohammadreza Azizi Amiri<sup>a</sup>

<sup>a</sup> Department of Organic Chemistry, Faculty of Chemistry, University of Mazandaran, Babolsar 47416-95447, Iran

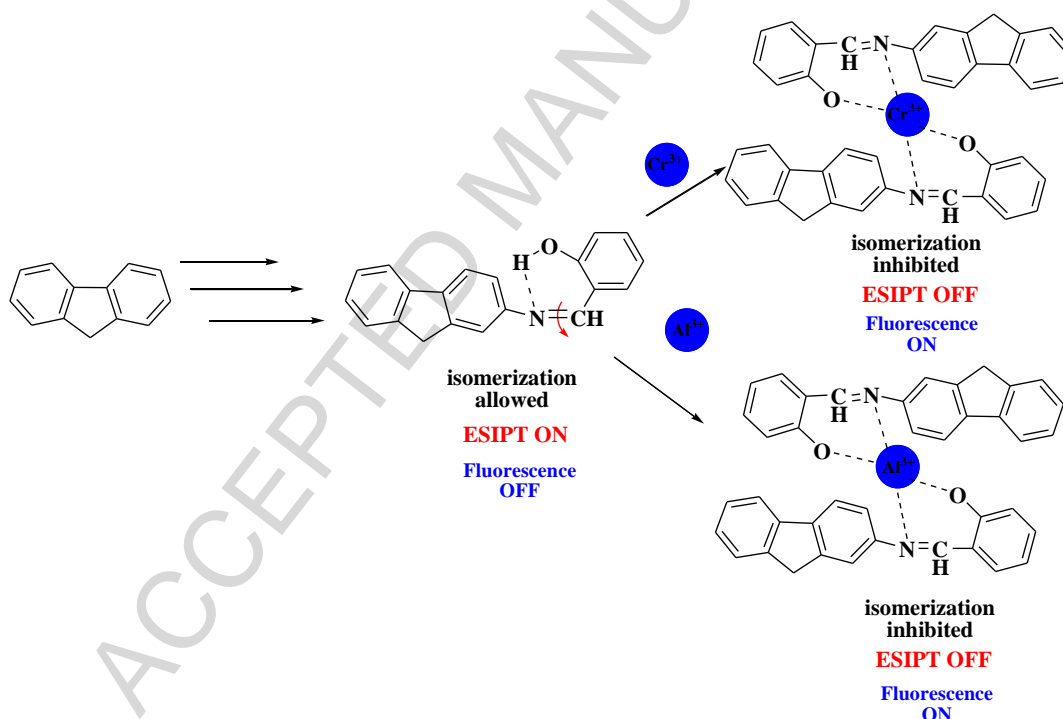
<sup>b</sup> Pharmaceutical Sciences Research Center, Department of Medicinal Chemistry, Mazandaran University of Medical Sciences, Sari, Iran

E-mail: Mahmood.Tajbakhsh32@gmail.com

Fax: +98 112 5242002

Tel: +98 112 5342301

## Graphical Abstract



## Highlights

- A novel fluorene-based Schiff-base sensor for  $\text{Cr}^{3+}$  and  $\text{Al}^{3+}$  ions has been designed, synthesized, and characterized.

- DFT calculations together with the experimental results obtained from Job's plot method showed a 2:1 binding ratio for both  $\text{Cr}^{3+}$  and  $\text{Al}^{3+}$  with Schiff base **F3**.
- The sensing mechanism is explained by excited state intra-molecular proton transfer (ESIPT) and C=N isomerization.
- The association constants ( $K_a$ ) for  $\text{Cr}^{3+}$  and  $\text{Al}^{3+}$  were calculated and found to be  $8.33 \times 10^4 \text{ M}^{-1}$  and  $5.44 \times 10^4 \text{ M}^{-1}$ , respectively.
- The detection limit of sensor towards  $\text{Cr}^{3+}$  and  $\text{Al}^{3+}$  were  $2.5 \times 10^{-7} \text{ mol/L}$  and  $3.1 \times 10^{-7} \text{ mol/L}$ , respectively.

### Abstract

2-((9H-fluoren-2-ylimino) methyl)phenol (**F3**) was synthesized by condensation reaction of 9H-fluoren-2-amine and 2-hydroxybenzaldehyde in EtOH and characterized by its melting point,  $^1\text{H}$ -,  $^{13}\text{C}$ -NMR and molecular mass. **F3** exhibits a high selectivity for detection of  $\text{Cr}^{3+}$  and  $\text{Al}^{3+}$  ions as a fluorescent chemosensor and showed a single emission band at 536 nm upon excitation at 333 nm according to fluorescence emission studies. The addition of  $\text{Cr}^{3+}$  and  $\text{Al}^{3+}$  make a significant increase in fluorescent intensity at 536 nm in  $\text{CH}_3\text{CN}$ , while other metal ions have almost no influence on the fluorescence. The fluorescence enhancement was attributed to the inhibited C=N isomerization and the obstructed excited state intra-molecular proton transfer (ESIPT) of compound **F3**. Job's plot and DFT calculations data showed that the binding stoichiometries of **F3** with  $\text{Cr}^{3+}$  and  $\text{Al}^{3+}$  are 2:1. The association constants ( $K_a$ ) for  $\text{Cr}^{3+}$  and  $\text{Al}^{3+}$  were calculated and found to be  $8.33 \times 10^4 \text{ M}^{-1}$  and  $5.44 \times 10^4 \text{ M}^{-1}$ , respectively. The detection

limits were also calculated for  $\text{Cr}^{3+}$  and  $\text{Al}^{3+}$  and found to be  $2.5 \times 10^{-7}$  mol/L and  $3.1 \times 10^{-7}$  mol/L, respectively.

*Keywords:* Fluorescence, Chemosensor, Chromium and Aluminum ions, ESIPT, Schiff-base, DFT

## 1. Introduction

Fluorescent chemosensors have received considerable attention, as they provide a convenient way for detection of metal ions [1–4]. Aluminum is one of the most abundant metals in the earth and is widely dispersed and used in the environment [5]. Nevertheless, as a non-essential and toxic element for living systems, the incremental increase of  $\text{Al}^{3+}$  concentrations is harmful to plant growth. Furthermore, exposure of the human body to high concentration of  $\text{Al}^{3+}$  is hazardous to health and can lead to a wide variety of diseases, such as Alzheimer, osteoporosis and etc [6–8]. The average daily intake of aluminum in humans is around 3–10 mg as reported by World Health Organization (WHO) [9]. Therefore, development of convenient and selective methods for determination of  $\text{Al}^{3+}$  is highly desirable [10]. As an essential heavy metal, chromium plays a vital role in the metabolism of carbohydrates, proteins, lipids and nucleic acids in biological systems [11]. The deficiency of chromium in the diet will increase risk factors associated with diabetes and cardiovascular diseases [12]. Chromium has also realized as a wide application in various industries such as pigment manufacturing, leather tanning, wood treatment and dyeing [13]. So, its importance toxic effects of  $\text{Cr}^{3+}$  and  $\text{Al}^{3+}$  in living systems leads to a growing interest in the development of appropriate analytical methods for their qualitative and quantitative detection in different biological and environmental samples. Although, the conventional techniques such as flame atomic absorption spectroscopy (FAAS) [14], inductively coupled plasma atomic emission spectroscopy (ICP-AES) [15], etc. Have been extensively employed for determination of  $\text{Cr}^{3+}$  and  $\text{Al}^{3+}$ , they are costly, complicated and not convenient for routine monitoring of  $\text{Cr}^{3+}$  and  $\text{Al}^{3+}$ . Thus, significant efforts have been considered for using of the fluorescent chemosensors to provide an easy and quick analysis of these elements [16-17]. Up to now, fluorene derivatives are mostly used for photoelectric functional materials and there are a few reports on fluorescent chemosensor of the fluorene derivatives for selective recognition of the metal ions [18-20]. Moreover,  $\text{Cr}^{3+}$  and  $\text{Al}^{3+}$  ions are well-known fluorescence quenchers due to their paramagnetism, which could affect the information of ‘turn-on’ fluorescent sensors

for their detection [21-23]. Many studies have been reported on designing turn on sensors because turn-off sensors usually produce a low signal output upon binding making them liable to interfere with the temporal separation of similar complexes with time-resolved fluorometry [24-27]. Different kinds of mechanisms such as photoinduced electron transfer (PET), metal to ligand charge transfer (MLCT), internal charge transfer (ICT), photoinduced proton transfer (PPT), excited state intra-molecular proton transfer (ESIPT), chelation-enhanced fluorescence (CHEF) effect and imine bond isomerization have been employed for designing fluorescent chemosensors [28–33]. Schiff bases that can be easily prepared by condensation of different types of amines and aldehydes have found widespread applications in coordination chemistry [34]. Schiff bases bearing a bridged C=N structure could easily isomerize in the excited state and tend to exhibit very weak fluorescence due to the C=N isomerization [35, 36]. However, the C=N isomerization is inhibited when this functional group can coordinate to metal ions to form the complexes that results in much stronger fluorescence signals. The ESIPT process usually involves the transfer of a proton donor (–OH, –NH<sub>2</sub>) to an adjacent proton acceptor (–C=O, –N=) through a six-membered ring of hydrogen-bonding configuration. In the presence of Cr<sup>3+</sup> and Al<sup>3+</sup>, the proton of the donor will be removed due to strong resonance-assisted hydrogen bonding (RAHB) and, as a result, the excited-state intra-molecular proton transfer process is inhibited and a significant emission increment or decrement can be observed [37-41]. In continuation of our studies on developing novel chemosensors [42-46], we report here the design and synthesis of a new fluorene-based Schiff-base (**F3**) which was synthesized by condensation of 9H-fluoren-2-amine and 2-hydroxybenzaldehyde (Scheme 1). Chelation of the resulting Schiff-base, 2-((9H-fluoren-2-ylimino)methyl)phenol (**F3**), with Cr<sup>3+</sup> and Al<sup>3+</sup>, inhibited the ESIPT process and C=N isomerization and showed a great fluorescence enhancement with turn-on at 536 nm, which is attributed to the formation of a 2:1 stoichiometric complex in acetonitrile.

## 2. Experimental

### 2.1. General and reagents

Melting points were measured on an Electrothermal 9100 apparatus. <sup>1</sup>H and <sup>13</sup>C spectra were measured with Bruker DRX-400 AVANCE spectrometer at 400.1 and 100.6 MHz, respectively. Mass spectra were obtained on an Agilent 5975c spectrometer operating at 70 eV. The UV-Vis

spectra were obtained using a Perkin-Elmer lambda-EZ 201 and a Jasco FP-200 spectra fluorometer was used to record fluorescence emission spectra. Data were recorded on-line and analyzed by Excel software on a PC computer. Fluorescence intensity measurements were performed at room temperature in CH<sub>3</sub>CN.

## 2.2. Synthesis

### 2.2.1. Synthesis of 2-nitro-9H-fluorene (**F1**)

Fluorene (60 g, 361 mmol) and 500 mL AcOH were added to a 1 L three-necked flask equipped with a thermometer and addition funnel. The reaction mixture was heated to 50 °C under nitrogen atmosphere. Then, nitric acid (80 mL) was added over 20 min via the addition funnel. The temperature was subsequently raised to 85 °C and maintained for 5 min. The resulting mixture was removed from the heater and then permitted to cool to room temperature over 2 h. Then, the resulting yellow suspension was filtered, washed with 50 mL AcOH containing 1.3 g KOAc, slurried in water and filtered again. The yellow product was dried in a vacuum oven, affording 58 g (77% yields) of desired product. The melting point was 152–158 °C. (Lit 155–156°C) [47]. <sup>1</sup>H NMR (400 MHz, CDCl<sub>3</sub>), δ, ppm: 8.42 (1H, d, J=1.2 Hz), 8.31 (1H, dd, J=2Hz, J=8Hz), 7.90-7.87 (2H, m), 7.65-7.62 (1H, m), 7.49-7.43 (2H, m), 4.01 (2H, S). <sup>13</sup>C NMR (100 MHz, CDCl<sub>3</sub>), δ, ppm: 148.08, 146.74, 144.82, 143.92, 139.46, 128.87, 127.43, 125.43, 123.13, 121.34, 120.48, and 119.88. The mass spectrum show peak at m/z = 211.1 corresponding to compound **F1** (Fig. S1-S2).

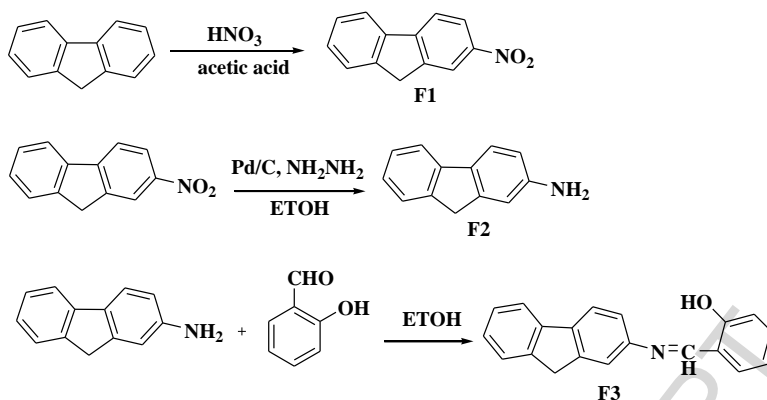
### 2.2.2. Synthesis of 9H-fluoren-2-amine (**F2**)

In a two-necked round-bottomed flask (500 ml) equipped with a reflux condenser and a dropping funnel, a suspension of 2-nitro-9H-fluorene (10.12 g, 48 mmol), palladium on carbon 5% (5 g), and ethanol (250 mL) was prepared. The mixture was heated, and while being stirred

magnetically, hydrazine hydrate 85% (35 ml) in ethanol (50 ml) was added dropwise over a 1.5 h period through the dropping funnel while maintaining the temperature at about 50 °C. The reaction mixture was then refluxed for 2 h and filtered while hot. On cooling, the filtrate gave light yellow colored crystals of the title diamine compound, which was recrystallized from ethanol and dried under vacuum to give 5.4 g (62% yield) (Scheme1). mp 129-134 °C. <sup>1</sup>H NMR (400 MHz, CDCl<sub>3</sub>), δ, ppm: 7.66 (1H, d, J=7.6 Hz), 7.59 (1H, d, J=8 Hz), 7.49 (1H, d, J=7.6 Hz), 7.36-7.32 (1H, m), 7.22 (1H, ddd, J=1.2 Hz, J=7.6 Hz), 6.91 (1H, t, J=0.4 Hz), 6.74 (1H, dd, J=2Hz, J=8 Hz), 3.83 (2H, S), 3.76 (2H, S, NH<sub>2</sub>). <sup>13</sup>C NMR (100 MHz, CDCl<sub>3</sub>), δ, ppm: 145.74, 145.16, 142.26, 142.14, 133, 126.63, 125.08, 124.75, 120.66, 118.58, 113.97, and 111.81. The mass spectrum show peak at m/z = 181.1 corresponding to compound **F2** (Fig. S3-S4).

### 2.2.3. Synthesis of 2-((9H-fluoren-2-ylimino)methyl)phenol (**F3**)

A solution of 9H-fluoren-2-amine (0.181 g, 1 mmol) in absolute ethanol was added to an ethanol solution of 2-hydroxybenzaldehyde (0.122 g, 1 mmol). The mixture was refluxed for 2 h and then cooled to room temperature. The solvent was evaporated and the yellow product was recrystallized from ethanol to yield 0.23 g (81%) of **F3** was (Scheme1). mp 142-147 °C. <sup>1</sup>H NMR (400 MHz, CDCl<sub>3</sub>), δ, ppm: 13.43 (1H, S), 8.74 (1H, S), 7.84 (2H, t, J=8.4 Hz), 7.76 (1H, d, J=7.2 Hz), 7.52 (1H, d, J=1.2 Hz), 7.45-7.38 (3H, m), 7.37-7.32 (2H, m), 7.06 (1H, d, J=8.4 Hz), 6.99 (1H, ddd, J=1.2 Hz, J=7.2 Hz), 3.94 (2H, S). <sup>13</sup>C NMR (100 MHz, CDCl<sub>3</sub>), δ, ppm: 161.70, 161.16, 147.19, 144.63, 143.43, 141.08, 140.81, 133.01, 132.19, 126.95, 126.85, 125.09, 120.56, 120.36, 119.94, 119.37, 119.08, 117.84 and 117.25. The mass spectrum show peak at m/z = 285.1 corresponding to compound **F3** (Fig. S5-S6).



**Scheme 1.** The synthetic route of compound **F3**.

### 2.3. Spectrometric procedure

Stock solutions ( $10\ \mu\text{M}$ ) of nitrate salts of  $\text{Na}^+$ ,  $\text{K}^+$ ,  $\text{Bi}^{2+}$ ,  $\text{Hg}^{2+}$ ,  $\text{Co}^{2+}$ ,  $\text{Cu}^{2+}$ ,  $\text{Zn}^{2+}$ ,  $\text{Cr}^{3+}$ ,  $\text{Cd}^{2+}$ ,  $\text{Fe}^{3+}$ ,  $\text{Al}^{3+}$  and  $\text{Ag}^+$  in  $\text{CH}_3\text{CN}$  were prepared. A solution of Schiff-base (**F3**) ( $10\ \mu\text{M}$ ) in acetonitrile was also prepared. Test solutions were prepared by placing 2 mL of the probe stock solution into cuvettes, adding 2 mL of each metal ion stock. For all measurements, excitation wavelength was at 333 nm.

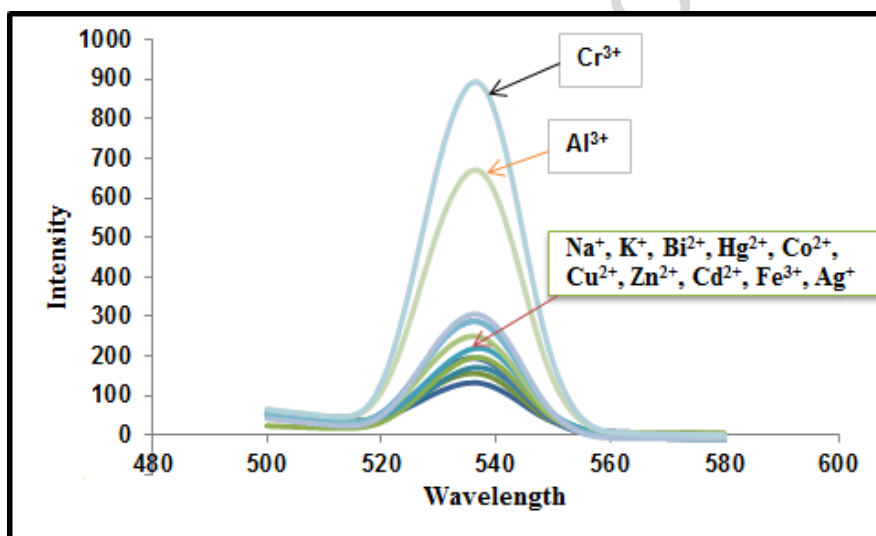
## 3. Results and discussion

### 3.1. Spectral studies

Fig. S7 and Fig.1 show the changes in the absorption and fluorescence spectra of **F3** in  $\text{CH}_3\text{CN}$  solution, upon the addition of various cation salts. The absorption spectrum of **F3** ( $10\ \mu\text{M}$ ) exhibits three bands at 228 nm, 330 nm and 363 nm. The absorption intensity of **F3** decreased with the addition of various heavy metal ions and  $\text{Cr}^{3+}$  and  $\text{Al}^{3+}$ . In all the cases, a hypochromic effect in the UV-Vis absorption spectra of **F3** was observed (Fig. S7). Because of the ambiguous absorption spectra, it was difficult to identify specific cations over other metal ions by UV-Vis analysis [48]. Therefore, to investigate the selectivity of **F3** for  $\text{Cr}^{3+}$  and  $\text{Al}^{3+}$  in the presence of other metal ions, the fluorescence response of **F3** toward various metal ion

solutions (10  $\mu\text{M}$ ) was studied in  $\text{CH}_3\text{CN}$  (Fig. 1). The fluorescence emission intensity of **F3** was recorded at 536 nm when it was excited at 333 nm. Upon addition of  $\text{Cr}^{3+}$  and  $\text{Al}^{3+}$ , **F3** shows a large fluorescence enhancement at 536 nm. The reason for this phenomenon is attributed to the formation of a 2:1 complex, resulted from the cation-induced inhibition of the excited state intramolecular proton transfer (ESIPT) process and C=N isomerization [35-41]. Other metal ions including  $\text{Na}^+$ ,  $\text{K}^+$ ,  $\text{Bi}^{2+}$ ,  $\text{Hg}^{2+}$ ,  $\text{Co}^{2+}$ ,  $\text{Cu}^{2+}$ ,  $\text{Zn}^{2+}$ ,  $\text{Cd}^{2+}$ ,  $\text{Fe}^{3+}$  and  $\text{Ag}^+$  had almost no influence on the fluorescence.

a)



b)

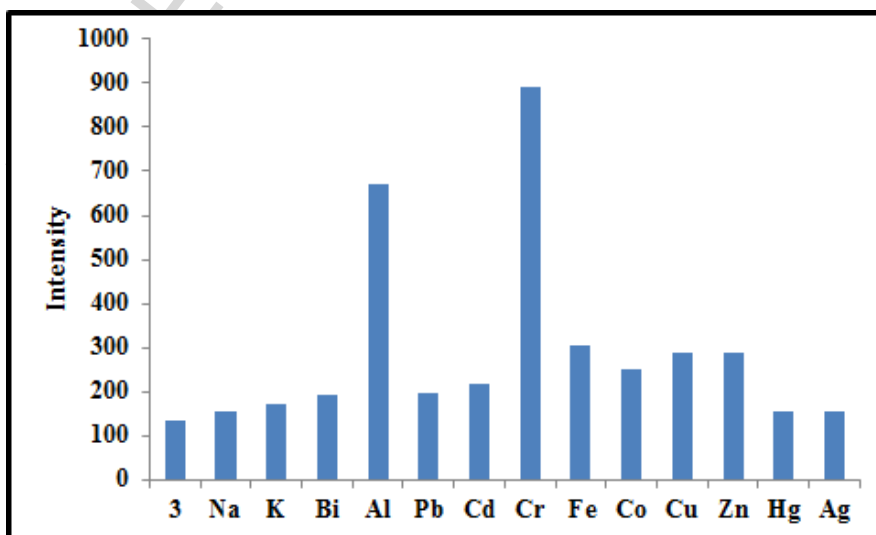


**Fig. 1.** (a) Fluorescence responses of compound **F3** (10 $\mu$ M) in CH<sub>3</sub>CN solution upon the addition of various metal ions (excitation = 333 nm, 2 equiv). (b) Bar graph representing the change of the relative emission intensity of **F3** at 536 nm upon treatment with various metal ions ( $\lambda_{ex}$  = 333 nm).

To explore the selectivity of **F3** for Cr<sup>3+</sup> and Al<sup>3+</sup>, the absorption in a mixture of other metal ions was measured in solution of CH<sub>3</sub>CN, resulted in a significant fluorescence intensity enhancement (Fig. 2). These observations demonstrated that compound **F3** could be used as an efficient and selective fluorescence chemosensor for Cr<sup>3+</sup> and Al<sup>3+</sup> ions.

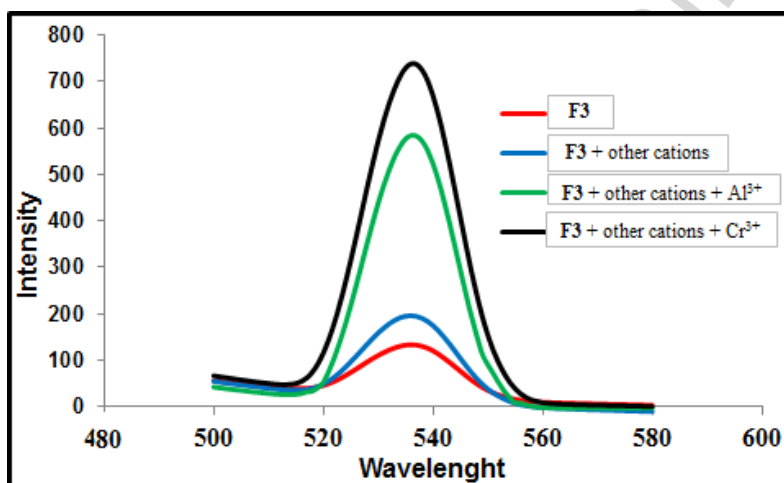


**Fig. 2.** Fluorescence intensity of **F3** (10  $\mu$ M) in the absence of metal ions (red curve), and presence of 2 equiv. of all kinds of competitive metal ions (blue curve) in CH<sub>3</sub>CN ( $\lambda_{ex}$  = 333 nm). The green curve represents the addition of Al<sup>3+</sup> to the above mixture. The black curve represents the addition of Cr<sup>3+</sup> to the above mixture. Each spectrum was acquired 1 minute after cations addition at room temperature.

To further investigate, the chemosensing properties of receptor **F3**, the fluorescence titration of **F3** with Cr<sup>3+</sup> and Al<sup>3+</sup> were performed. By increasing the concentrations of Cr<sup>3+</sup> and Al<sup>3+</sup>, the sensitivity of **F3** (10  $\mu$ M) in CH<sub>3</sub>CN towards Cr<sup>3+</sup> and Al<sup>3+</sup> ions were clearly observed in Fig. 3. The fluorescence spectrum of **F3** ( $\lambda_{em}$ =536 nm) showed rapid turn-on responses and the inset illustrated relative fluorescence intensity changes as a function of Cr<sup>3+</sup> and Al<sup>3+</sup> concentration.

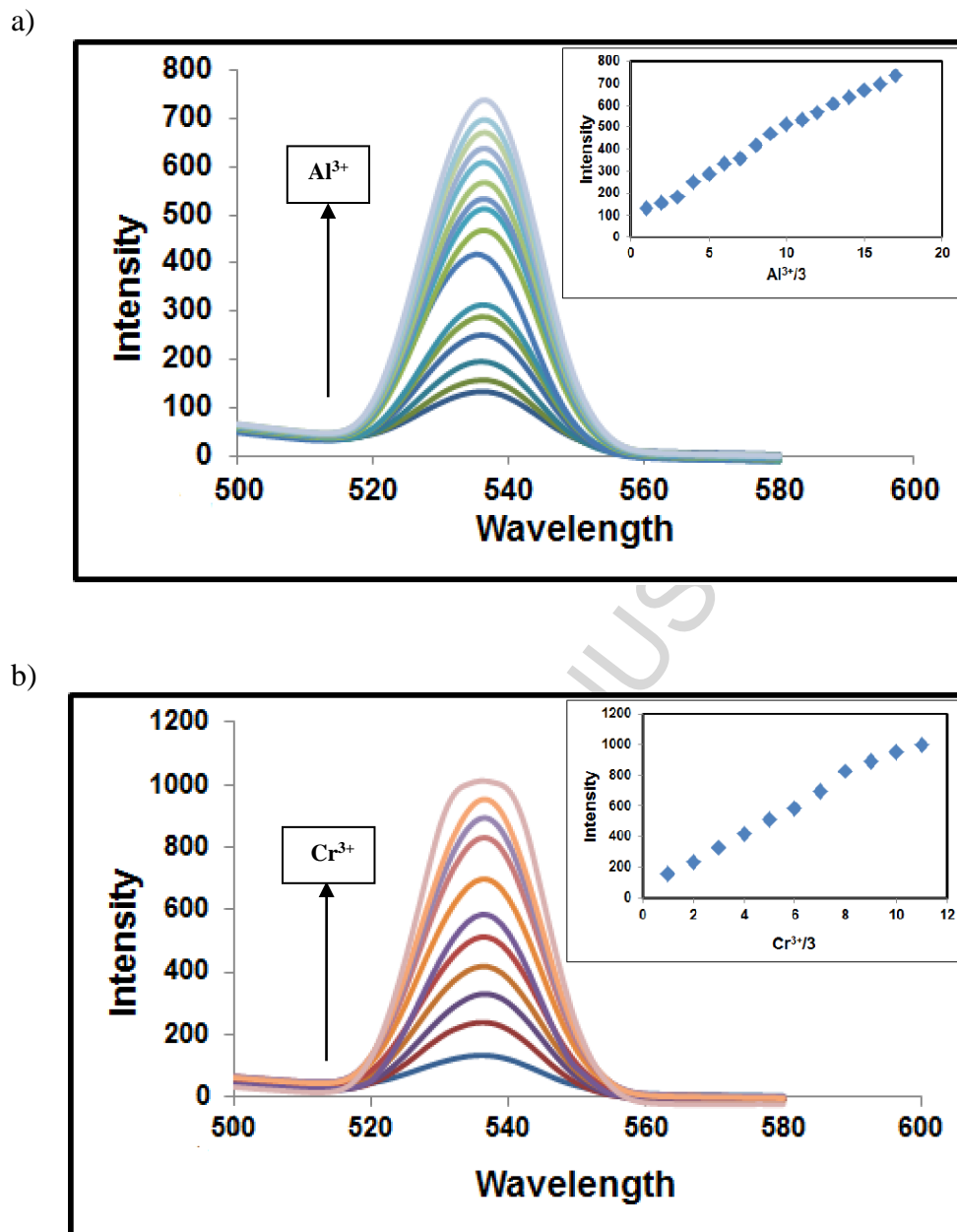


**Fig. 3.** (a) Fluorescence titration of **F3** (10  $\mu$ M) with various concentration of  $\text{Al}^{3+}$  (0-2 equiv) in  $\text{CH}_3\text{CN}$  solution (excitation = 333 nm); inset: changes of fluorescence upon addition of  $\text{Al}^{3+}$  at emission=536 nm. (b) Fluorescence titration of **F3** (10  $\mu$ M) with various concentration of  $\text{Cr}^{3+}$  (0-2 equiv) in  $\text{CH}_3\text{CN}$  solution (excitation = 333 nm); inset: changes of fluorescence upon addition of  $\text{Cr}^{3+}$  at emission=536 nm.

The association constant ( $K_a$ ) of compound **F3** with metal ions was determined using the Benesi–Hildebrand equation [49] as follows:

$$\frac{1}{F - F_0} = \frac{1}{K_a(F_{\max} - F_0)[M]} + \frac{1}{F_{\max} - F_0}$$

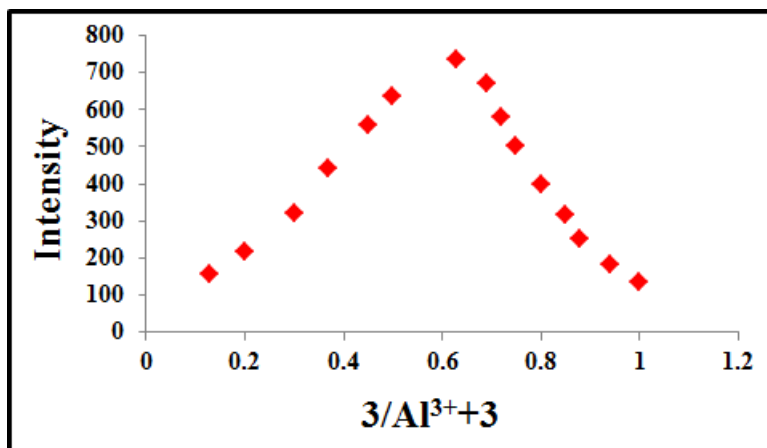
F and  $F_0$  represent the fluorescence intensity of compound **F3** in the presence and absence of metal ions, respectively.  $F_{\max}$  indicates the saturated fluorescent intensity of **F3** in the presence of excess amounts of metal ions. [M]. Using the Benesi–Hildebrand equation, the association constants for **F3**-Cr<sup>3+</sup> and **F3**-Al<sup>3+</sup> were calculated from the fluorescence titration results and obtained  $8.33 \times 10^4 \text{ M}^{-1}$  and  $5.44 \times 10^4 \text{ M}^{-1}$  respectively. Furthermore, the limitation of detection was calculated according to fluorescence titration. To determine the S/N ratio, the emission intensity of the complexes (**F3**-Cr<sup>3+</sup> and **F3**-Al<sup>3+</sup>) were measured and the standard deviation of blank measurements were calculated. The limitation of detection was then calculated according to  $3 \times \delta b/m$ , where  $\delta b$  is the standard deviation of blank solutions, and "m" is the slope between intensity versus sample concentration [50]. The detection limits for Cr<sup>3+</sup> and Al<sup>3+</sup> were calculated to be  $2.5 \times 10^{-7} \text{ mol/L}$  and  $3.1 \times 10^{-7} \text{ mol/L}$ , respectively. Fluorescence quantum yield was measured by assessment the emission and absorption intensities of the probe in respect to those of a fluorescence standard, fluorescein in 0.1 N NaOH. For all fluorescence measurements, the excitation wavelength was 333 nm with excitation and emission slit widths of 3.0 nm. Accordingly, the quantum yields of 14.8% and 12.9% were determined for the **F3**-Cr<sup>3+</sup> and the **F3**-Al<sup>3+</sup> complexes. However, low quantum yields were obtained for the combination of the receptor with other metal cations as well as for the free receptor and no worth to report. Ligand **F3** as a fluorescence probe can be widely used to measure the low concentrations ( $\sim \mu\text{M}$ ) of Cr<sup>3+</sup> and Al<sup>3+</sup> cations in biochemical chemical environmental and forensic analysis. The sensitivity of fluorescence detection is approximately one thousand times greater than absorption spectrophotometric methods. This means, the fluorimetry may even be a more powerful method for Cr<sup>3+</sup> and Al<sup>3+</sup> cations characterization than UV/Vis spectrophotometry. Leading greater limits of detection, while potentially using less Cr<sup>3+</sup> and Al<sup>3+</sup> cations. It might be important especially when working with valuable or limited-quantity of the cations.

### 3.2. Binding mode studies

The stoichiometric relationship between the ligand **F3** with Cr<sup>3+</sup> and Al<sup>3+</sup> were confirmed by the Job's plot. The intensity of fluorescence emission was measured by varying the mole fraction of **F3**. As shown in Fig. 4, the fluorescence emission intensity showed a maximum when

the molar fraction of **F3** were 0.67, demonstrates the formation of 2:1 ratio of **F3** with  $\text{Cr}^{3+}$  and  $\text{Al}^{3+}$ .

a)



b)

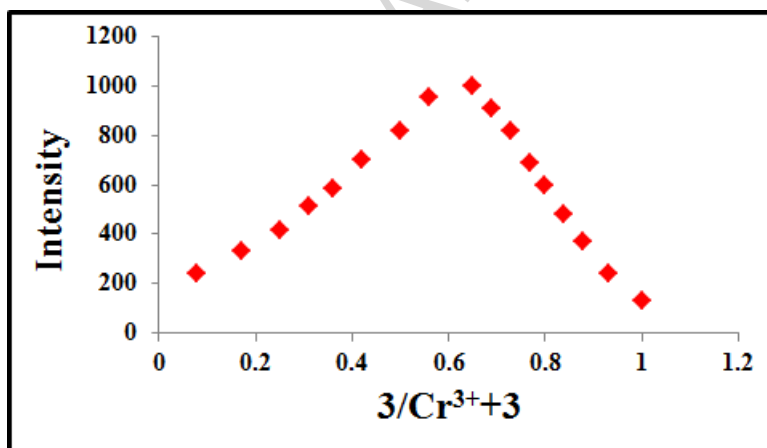
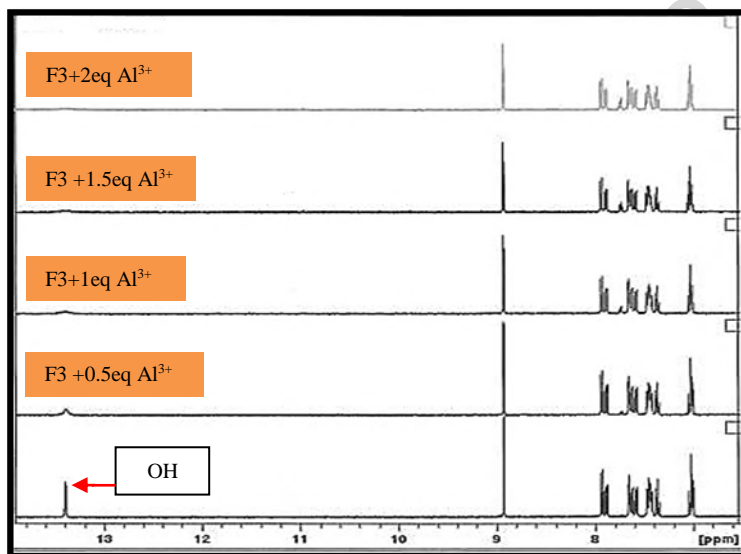


**Fig. 4.** Job's plot titration of **F3** with  $\text{Al}^{3+}$ , the total concentration of **F3** and  $\text{Al}^{3+}$  is  $10\ \mu\text{M}$  (a) and  $\text{Cr}^{3+}$ , the total concentration of **F3** and  $\text{Cr}^{3+}$  is  $10\ \mu\text{M}$  (b) at room temperature.

In order to get further insight into the binding event of **F3** with  $\text{Cr}^{3+}$  and  $\text{Al}^{3+}$ ,  $^1\text{H}$  NMR spectra of **F3** in the absence and presence of  $\text{Cr}^{3+}$  and  $\text{Al}^{3+}$  were measured in  $\text{CD}_3\text{CN}$  (Fig. 5). The Proton shift of **F3** at 13.43 ppm can be assigned to the hydroxyl proton, which is involved in the intra-molecular hydrogen bond ( $\text{OH}\dots\text{N}$ ) [51]. The phenolic hydroxyl proton at 13.43 ppm disappeared when 2 equiv of  $\text{Cr}^{3+}$  and  $\text{Al}^{3+}$  were added to the **F3** solution. This observation

implies that the phenolic OH groups are involved in the formation of complex between the **F3** with  $\text{Cr}^{3+}$  and  $\text{Al}^{3+}$  [52]. The signals of other protons in **F3** and complexes did not show any significant change. The binding mode of **F3** with  $\text{Cr}^{3+}$  and  $\text{Al}^{3+}$  is meaningful for the design of new  $\text{Cr}^{3+}$  and  $\text{Al}^{3+}$  fluorescent chemosensors.

a)



b)

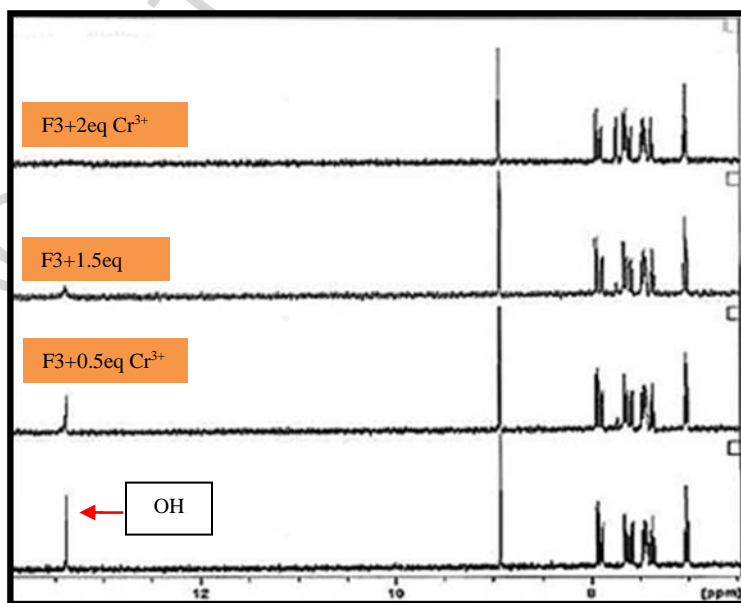


**Fig. 5.**  $^1\text{H}$  NMR spectra of **F3** (10  $\mu\text{M}$ ) with  $\text{Al}^{3+}$  and  $\text{Cr}^{3+}$  in  $\text{CD}_3\text{CN}$ : (a) **F3** and  $\text{Al}^{3+}$  (0-2 equiv) (b) **F3** and  $\text{Cr}^{3+}$  (0-2 equiv). Each spectrum was acquired 1 minute after cations addition at room temperature.

### 3.3. Theoretical study

#### 3.3.1. The optimization studies

The given complexes (**F3**– $\text{Al}^{3+}$  and **F3**– $\text{Cr}^{3+}$ ) have produced as fine powders, so far we were not able to obtain the single crystals of the compounds to determine the electronic structures by X-ray crystallography [10]. To get insight into the proposed binding modes, the full geometry optimizations were performed without any symmetry constraints by density functional calculations (DFT) [53] in the framework of the Becke three-parameter hybrid exchange and Lee–Yang–Parr correlation functional (B3LYP), employing Gaussian 09 package [54]. Whole the atoms were characterized by a split-valence Pople basis set plus polarization and diffuse functions, 6-31+G (d, p), but a double- $\zeta$  quality LANL2DZ basis set was employed for both Cr (III) and Al (III) atoms. The optimized structure of the **F3** Schiff base and its complexes are shown in Fig 6, indicating 2:1 stoichiometry between the sensor **F3** and  $\text{Cr}^{3+}/\text{Al}^{3+}$ . Also, the selected calculated bond distances and the bond angles are shown in Table 1. As shown in Fig. 6, the coordination environments around both Cr (III) and Al (III) are tetrahedral with some distortion, by nitrogen atoms of imine groups (N1 and N2) and two deprotonated phenolic oxygens (O1 and O2). The calculated bond angles show appreciable deviation from ideal tetrahedral value of  $109.5^\circ$ , suggesting that tetrahedral geometry is slightly distorted due to chelation effects.

To find the mole percent of the sensor to moles of the metal, the fluorescence titration experiments were performed using 10  $\mu\text{M}$  of **F3** with varying concentrations of  $\text{Cr}^{3+}$  and  $\text{Al}^{3+}$  in solution  $\text{CH}_3\text{CN}$  which are shown a relationship between absorbance and mole ratio of 2:1, consistent with the theoretical results.

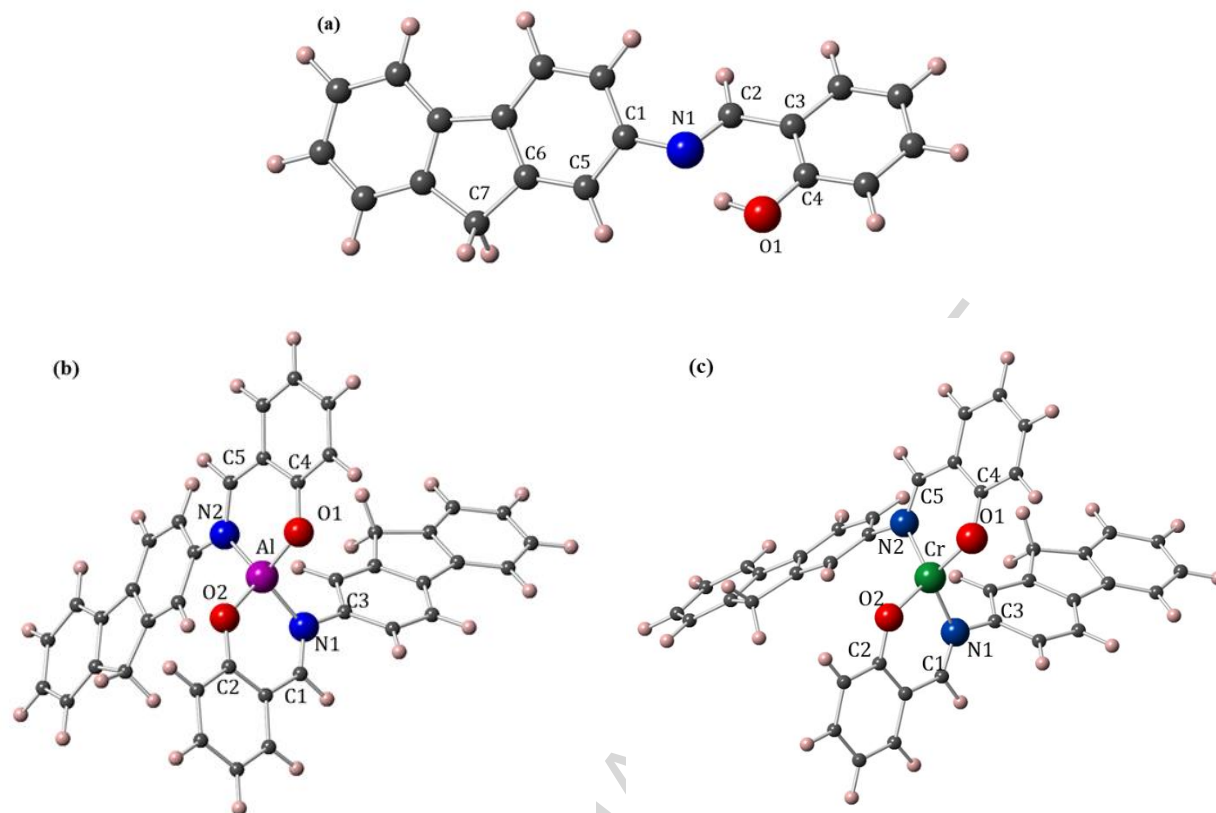


**Fig. 6.** The optimized structures of the **F3** (a), **F3–Al<sup>3+</sup>** (b) and **F3–Cr<sup>3+</sup>** (c).

**Table 1:** Selected bond lengths (Å) and bond angles  $\angle(^{\circ})$  for the structures of **F3** (ligand), **F3–Al<sup>3+</sup>** and **F3–Cr<sup>3+</sup>**

<b>F3–Al</b>		<b>F3–Cr</b>		<b>F3</b>	
Al–O1	1.757	Cr–O1	1.833	N1–C1	1.407
Al–O2	1.775	Cr–O2	1.841	N1–C2	1.294
Al–N1	1.941	Cr–N1	1.999	O1–C4	1.344
Al–N2	1.933	Cr–N2	2.004	C2–C3	1.450
N1–C1	1.328	N1–C1	1.321	C3–C4	1.423
O2–C2	1.351	O2–C2	1.351	C1–C5	1.409
N1–C3	1.447	N1–C3	1.446	C5–C6	1.387
O1–C4	1.360	O1–C4	1.350	C6–C7	1.515
N2–C5	1.424	N2–C5	1.324	$\angle$ C1NC2	121.60
$\angle$ N2AlO1	99.90	$\angle$ N2 Cr O1	88.84	$\angle$ C3C4O	121.70
$\angle$ N1AlO2	95.94	$\angle$ N1 Cr O2	88.60	$\angle$ NC1C5	117.46
$\angle$ N1AlO1	109.71	$\angle$ N1 Cr O1	118.66	$\angle$ C1NC2C3	177.12
$\angle$ N2AlO2	113.35	$\angle$ N2CrO2	118.41	$\angle$ C1C5C6C7	179.13

### 3.3.2. The TD-DFT calculations

The excited-state electronic spectra of the **F3** (Schiff base) and the **F3-Al<sup>3+</sup>** and **F3-Cr<sup>3+</sup>** complexes, optimized with inclusion of acetonitrile solvent, were calculated by TDDFT/IEFPCM method to determine the energies and compositions of the molecular orbitals (MOs) [55]. The assignment of the most important occupied (HOMOs) and unoccupied (LUMOs) orbitals involved in electronic transitions in  $\alpha$  and  $\beta$  spin states in acetonitrile solvent, with the fragment Mulliken contributions expressed in terms of the compositions from the metal central atoms (Cr and Al), Fluorene-part (Flou), CN, Phenyl-part (Ph) and OH were presented in Fig 7. The HOMO orbital in Schiff base is mostly characterized with  $\pi$ -orbitals of Flou fragment but the LUMO is exhibited by a mixture of  $\pi^*$ -orbitals of CN (39%), Ph (32%) and Flou (27%) characters. In both  $\alpha$ - and  $\beta$ -spin states of the **F3-Cr<sup>3+</sup>**, the HOMOs are significantly composed with the  $\pi$  orbitals of Flou character, while the LUMOs, in  $\alpha$ -spin are importantly localized on Cr (64%) character and also in  $\beta$ -spin, are indicated of CN (39%), Cr (29%) and Ph (27%) characters. On the other hand, the HOMOs and LUMOs orbitals of the **F3-Al<sup>3+</sup>** in  $\alpha$ -spin state, are predominately composed by an admixture of  $\pi$ -character of Ph (34%) and CN (44%) contributions but in  $\beta$ -spin state, both HOMO and LUMO orbitals are composed with  $\pi$ - and  $\pi^*$ -characters of Flou (89% and 73%) fragments, respectively. As seen in Fig 7, both HOMO's and LUMO's energies in the **F3-Al<sup>3+</sup>** and **F3-Cr<sup>3+</sup>** compounds are more stabilized than the **F3-Schiff** base, so the **F3** can convenience convert to **F3-Al<sup>3+</sup>** and **F3-Cr<sup>3+</sup>** compounds by narrowing the energy gap between the HOMO and LUMO.

The theoretical UV-Vis spectra of the titled compounds in the ranges of 180-700 nm are shown in Figure 8. The d-d band pattern suggests that Cr (III) and Al (III) centers are distorted as a tetrahedral geometry. Generally, three possible d-d band expected for  $d^3$  configuration in a

tetrahedral geometry which are  ${}^4T_2(F) \rightarrow {}^4T_1(F)$ ,  ${}^4T_2(F) \rightarrow {}^4T_1(P)$  and  ${}^4T_2(F) \rightarrow {}^4A_2(F)$ . Thus, the theoretical absorption spectrum at 333.6 (shoulder), 387.9 and 515.4 nm for **F3**-Cr<sup>3+</sup> complex and the bands at 335.8, 422.9 and 569.5 nm for **F3**-Al<sup>3+</sup> complex are attributed to first, second and third ligand-field transitions, respectively. The exhibited electronic excited state at 326.0 nm corresponding to **F3** ligand are in agreement with the experimental spectrum at 333 nm together with its fluorescence emission recorded at 536 nm. By complexation of the **F3** ligand to Cr<sup>3+</sup> and Al<sup>3+</sup>, this excited spectrum is shifted to 333.6 nm (**F3**-Cr<sup>3+</sup>) and 335.8 nm (**F3**-Al<sup>3+</sup>), respectively (as shown in Figure 6). The major transitions at 333.6 nm (ligand) is due the electron transition from (HOMO-1) to (LUMO) orbitals which occur from dominant excitation characters of  $\pi$ -Phenyl (67%),  $\pi$ -OH (16%) and  $\pi$ -Flourene (16%) to  $\pi^*$ -Phenyl (32%),  $\pi^*$ -CN (39%) and  $\pi^*$ -Flourene (27%).

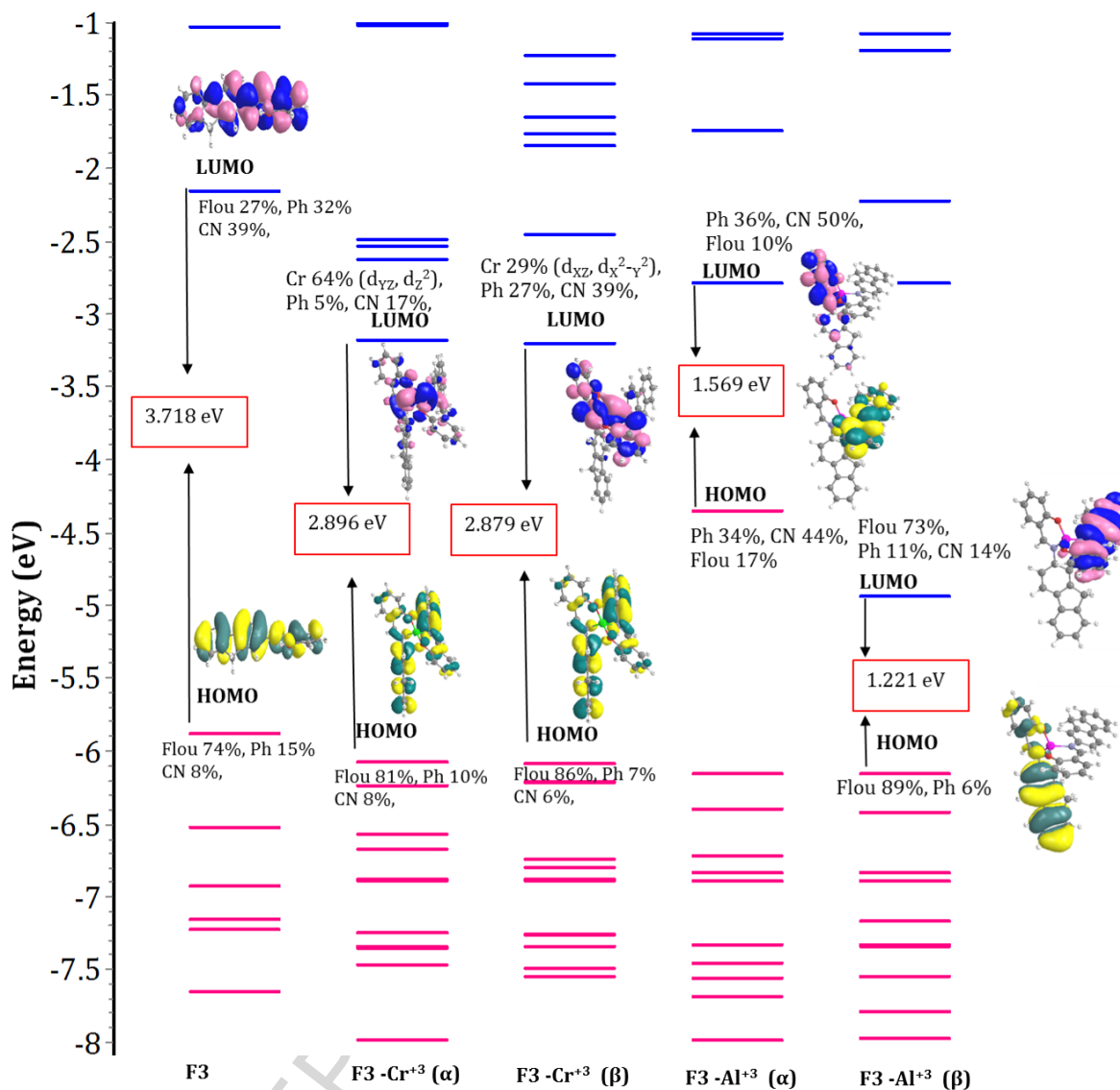


**Fig. 7.** The energy (eV), character and some contours of the HOMO and LUMO molecular orbitals of the compounds. Positive values of the HOMOs and LUMOs contour are represented in pink and yellow and the negative values in blue and green, respectively.

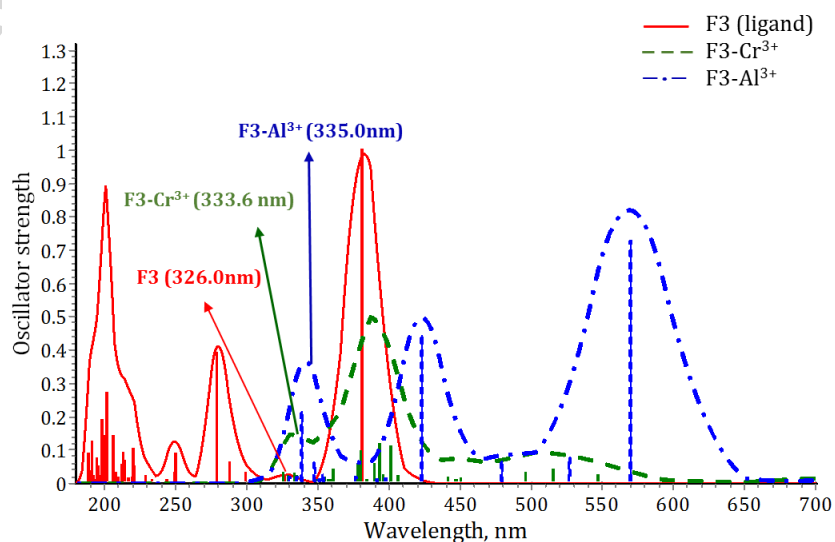
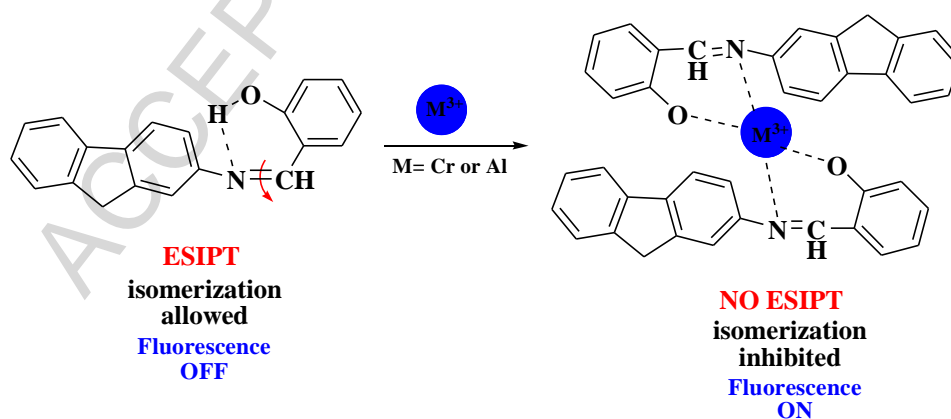


**Fig. 8.** The calculated UV-Vis spectra of the **F3** (red line), **F3–Al<sup>3+</sup>** (blue line) and **F3–Cr<sup>3+</sup>** (green line) compounds.

### 3.4. The proposed mechanism

According to the above experiments, it could be suggested that the **F3** chelates with  $\text{Cr}^{3+}$  and  $\text{Al}^{3+}$  through interactions with imine nitrogen and the oxygen of the phenolic hydroxyl groups [56–59]. The sensing mechanism was estimated using the degree of chelation. In solution, the free **F3** exhibited weak fluorescence emission because of ESIPT and C=N isomerization. The isomerization of C=N bond is the predominant decay process of the excited state for the compound **F3**. Upon addition of  $\text{Cr}^{3+}$  and  $\text{Al}^{3+}$  the compound **F3** coordinates with the metal ions and inhibits the C=N bond isomerization. The C=N isomerization mechanism for the Schiff-base receptors have been reported for detection of metal ions various types [60]. The coordination between  $\text{Cr}^{3+}$  and  $\text{Al}^{3+}$  with **F3** a deprotonates the phenolic hydroxyl groups preventing the intra hydrogen bonding with imine nitrogen (OH...N) and also inhibits the intra-molecular proton transfer in the excited state (Scheme 2) [61, 62]. This phenomenon has been confirmed by  $^1\text{H}$  NMR analysis as described in section (3. 2).



Scheme. 2. Proposed mechanism for detection of  $\text{Cr}^{3+}$  and  $\text{Al}^{3+}$  by **F3**.

### 3.5. Solvent effect

Optical sensing nature of chemosensors was found to be depended on the solvent nature, so the response of ligand **F3** toward  $\text{Cr}^{3+}$  ion was also examined in different solvents such as DMSO, DMF, methanol, acetonitrile, acetonitrile/ $\text{H}_2\text{O}$  at maxima of emission intensity. As showed in fig. 9, the optimum fluorescence enhancement occurred only in case of acetonitrile. The aprotic solvents (DMSO, DMF) and protic solvents (methanol,  $\text{H}_2\text{O}$ ) decrease significant the intensity of fluorescent, which might be due to hydrogen bonding of this solvents with hydroxyl groups, rather than general solvent effects [63]. However, the highest fluorescent intensity was observed in acetonitrile. So acetonitrile was chosen as solvent [64, 65].

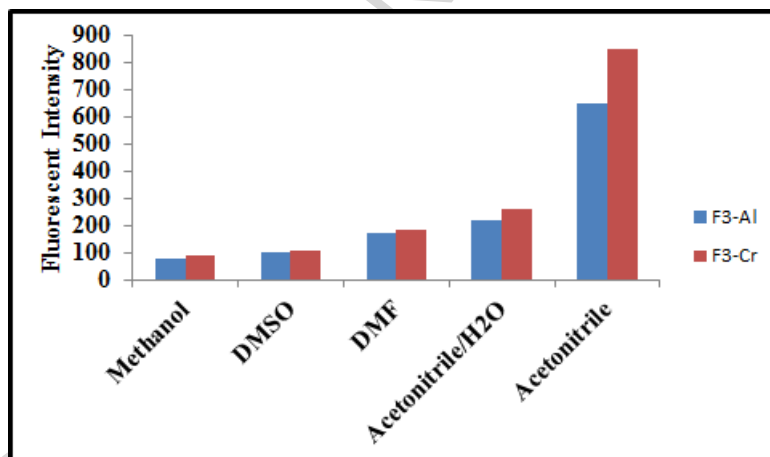


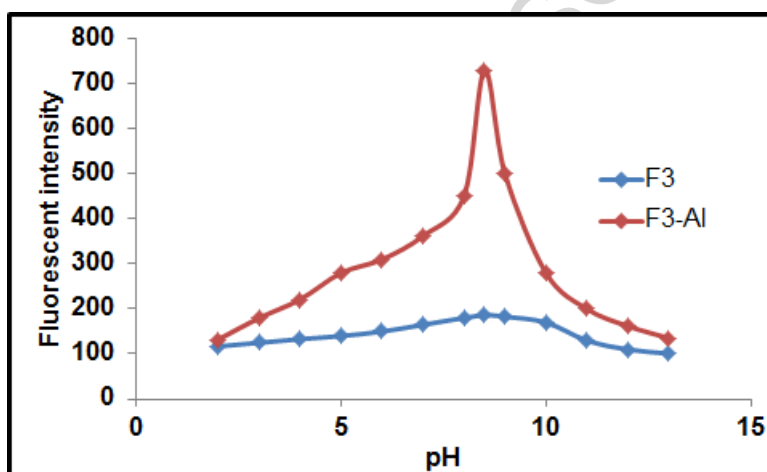
**Fig. 9.** Solvent effect on fluorescent intensity of **F3** (10  $\mu\text{M}$ ) with  $\text{Al}^{3+}$  (2 equiv) and  $\text{Cr}^{3+}$  (2 equiv) in different solvent methanol, DMSO, DMF, acetonitrile/ $\text{H}_2\text{O}$  and acetonitrile.

### 3.6. Effect of pH on the binding affinity of $\text{Cr}^{3+}$ to **F3**

Since pH of the medium plays a crucial role in fluorescence detection, the effect of pH in the range of (2–13) on the fluorescence response of **F3** was investigated in  $\text{CH}_3\text{CN}$ . The changes in the fluorescence intensity at 536 nm of **F3** in the absence and presence of  $\text{Cr}^{3+}$  and  $\text{Al}^{3+}$  ions were plotted as a function of pH (Fig. 10). The overall fluorescence intensity of **F3**– $\text{Cr}^{3+}$  and **F3**–

$\text{Al}^{3+}$  complexes remained higher than the free receptor **F3**. The highest fluorescent intensity was obtained at pH 8.5. The emission intensity was decreased over the pH 8.5, possibly due to the formation of  $\text{Cr}(\text{OH})_3$  and  $\text{Al}(\text{OH})_3$  that precipitate from the solution and will become unavailable to the chelating agent. Similarly, under the pH 8.5, **F3** might react with  $\text{H}^+$  and show slow affinity for binding to  $\text{Cr}^{3+}$  or  $\text{Al}^{3+}$ , resulting a decrease in fluorescence intensity. Therefore, **F3** can tolerate the detection of  $\text{Cr}^{3+}$  and  $\text{Al}^{3+}$  in the pH 8.5 [66].

a)



b)

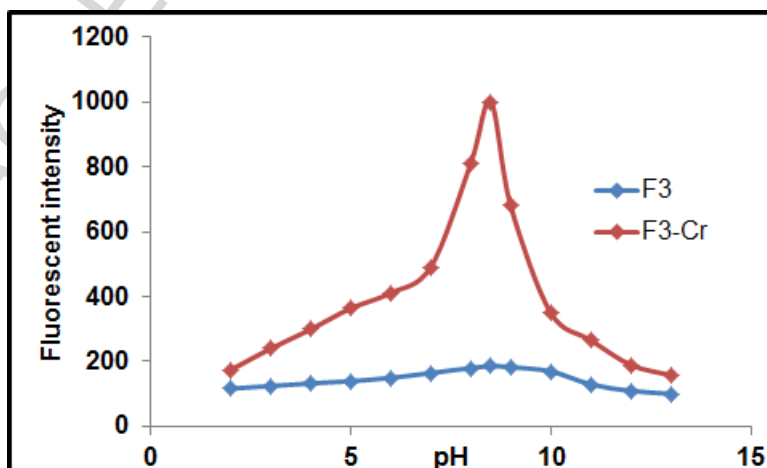


**Fig. 10.** Fluorescence response for **F3** (10  $\mu\text{M}$ ) in the absence and presence of  $\text{Al}^{3+}$  (2 equiv) (a) and  $\text{Cr}^{3+}$  (2 equiv) (b) as a function of pH in  $\text{CH}_3\text{CN}$  at 536 nm.

### 3.7. Comparison

The 2-((9H-fluoren-2-ylimino) methyl) phenol (**F3**) for fluorescence sensing of  $\text{Cr}^{3+}$  and  $\text{Al}^{3+}$  are very interesting. In addition, we compared the present sensor with those previously reported chemosensors for  $\text{Cr}^{3+}$  and  $\text{Al}^{3+}$  (Table 2). Chemosensor **F3** exhibited better response relatively.

**Table 2:** Comparative analysis of chemosensor **F3** with previously reported sensors.

Ionophores	mechanism	Methods of detections	Medium of detection	Detection limit (M)	Binding Constant $\text{M}^{-1}$	Sensing response	pH range
Ref. 67	-	fluorescent	$\text{CH}_3\text{CN}/\text{H}_2\text{O}$ (8:2)	$7.94 \times 10^{-5}$	$1.6 \times 10^4$	$\text{Cr}^{3+}$ (Turn on)	7
Ref. 68	ICT and CHEF	fluorescent	$\text{EtOH}/\text{H}_2\text{O}$ (3:7)	$3.20 \times 10^{-6}$	-	$\text{Al}^{3+}$ (Turn on)	7.4
Ref. 69	PET	colorimetric and fluorescent	MeOH	$1.21 \times 10^{-6}$	$1.01 \times 10^4$	$\text{Cr}^{3+}$ (Turn on)	2-7
Ref. 69	PET	colorimetric and fluorescent	MeOH	$7.3 \times 10^{-7}$	$2.63 \times 10^4$	$\text{Al}^{3+}$ (Turn on)	2-7
Ref. 70	-	colorimetric and fluorescent	MeOH	$1.1 \times 10^{-5}$	$1.4 \times 10^4$	$\text{Cr}^{3+}$ (Turn on)	-
Ref. 71	CHEF	fluorescent	$\text{EtOH}-\text{H}_2\text{O}$ (95:5)	$3.6 \times 10^{-6}$	$2 \times 10^4$	$\text{Al}^{3+}$ (Turn on)	-
Ref. 72	ESIPT and C=N isomerization	colorimetric and fluorescent	$\text{CH}_3\text{CN}$	$2.75 \times 10^{-6}$	$5.97 \times 10^4$	$\text{Cr}^{3+}$ (Turn on)	-
Ref. 73	MLCT	fluorescent	$\text{CH}_3\text{CN}$	$10^{-6}$	$1.14 \times 10^4$	$\text{Al}^{3+}$ (Turn on)	-
Ref. 74	-	fluorescent	$\text{CH}_3\text{CN}$	$9.86 \times 10^{-6}$	$2.1 \times 10^3$	$\text{Cr}^{3+}$ (Turn on)	6-8
Ref. 75	ICT	fluorescent	$\text{H}_2\text{O}/\text{CH}_3\text{CN}$	$10^{-6}$	13.98	$\text{Al}^{3+}$ (Turn on)	-
<b>F3</b>	ESIPT and C=N isomerization	fluorescent	$\text{CH}_3\text{CN}$	$2.5 \times 10^{-7}$	$8.33 \times 10^4$	$\text{Cr}^{3+}$ (Turn on)	8.5
<b>F3</b>	ESIPT and C=N isomerization	fluorescent	$\text{CH}_3\text{CN}$	$3.1 \times 10^{-7}$	$5.44 \times 10^4$	$\text{Al}^{3+}$ (Turn on)	8.5

## 4. Conclusion

In summary, a highly selective and sensitive fluorescent sensor based on fluorene derivative for detection of  $\text{Cr}^{3+}$  and  $\text{Al}^{3+}$  has been developed. The sensor **F3** shows a great fluorescence turn-on upon binding to  $\text{Cr}^{3+}$  or  $\text{Al}^{3+}$  that inhibits ESIPT and C=N isomerization. In addition, the binding

stoichiometry was confirmed as 2:1 (**F3**/Cr<sup>3+</sup>) and 2:1 (**F3**/Al<sup>3+</sup>) by Job's plot method together with theoretical study. The association constants ( $K_a$ ) for Cr<sup>3+</sup> and Al<sup>3+</sup> were calculated and found to be  $8.33 \times 10^4 \text{ M}^{-1}$  and  $5.44 \times 10^4 \text{ M}^{-1}$ , respectively. The detection limit of sensor towards Cr<sup>3+</sup> and Al<sup>3+</sup> were  $2.5 \times 10^{-7} \text{ mol/L}$  and  $3.1 \times 10^{-7} \text{ mol/L}$ , respectively exhibiting more efficient than other reported Cr<sup>3+</sup> and Al<sup>3+</sup> sensors [67–75]. However the present chemosensor system with the remarkable photophysical properties could extend applications of fluorescent sensor for Cr<sup>3+</sup> and Al<sup>3+</sup>.

## References

- [1] M.P. Yang, W.F. Meng, X.J. Liu, N. Su, J. Zhou, B.Q. Yang, *RSC Adv.* 4 (2014) 22288–22293.
- [2] Y.X. Gao, X. Li, Y.L. Li, T.H. Li, Y.Y. Zhao, A.G. Wu, *Chem. Commun.* 50 (2014) 6447–6450.
- [3] H. Liu, X. Hao, C.H. Duan, H. Yang, Y. Lv, H.J. Xu, H.D. Wang, F. Huang, D.B. Xiao, Z.Y. Tian, *Nanoscale.* 5 (2013) 9340–9347.
- [4] W.H. Hsieh, C.F. Wan, D.J. Liao, A.T. Wu, *Tetrahedron Lett.* 53 (2012) 5848–5851.
- [5] M. Iniya, D. Jeyanthi, K. Krishnaveni, A. Mahesh, D. Chellappa, *Spectrochim. Acta A.* 120 (2014) 40–46.
- [6] J. Tria, E.C.V. Butler, P.R. Haddad, A.R. Bowie, *Anal. Chim. Acta.* 588 (2007) 153–165.
- [7] K. Kaur, V.K. Bhardwaj, N. Kaur, N. Singh, *Inorg. Chem. Commun.* 18 (2012) 79–82.
- [8] G. Tamil Selvan, M. Kumaresan, R. Sivaraj, P. Mosae Selvakumar, *Sens. Actuators B.* 229 (2016) 181–189.
- [9] B. Valeur, I. Leray, *Coord. Chem. Rev.* 205 (2000) 3–40.
- [10] R. Azadbakht, S. Rashidi, *Spectrochim. Acta A.* 127 (2014) 329–334.
- [11] A.K. Singh, V.K. Gupta, B.H. Gupta, *Anal. Chim. Acta.* 585 (2007) 171–178.
- [12] R. McRae, P. Bagchi, S. Sumalekshmy, C.J. Fahrni, *Chem Rev.* 109 (2009) 4780–4827.
- [13] M.E. Losi, C. Amrhein, W.T. Frankenberger, *Rev. Environ. Contam. Toxicol.* 136 (1994) 91–121.
- [14] T. Shampur, I. Sheikhshoai, M.H. Mashhadizadeh, *J. Anal. At. Spectrom.* 20 (2005) 476–478.
- [15] P. Vanlout, B. Coulomb, C. Brach-Papa, M. Sergent, J.L. Boudenne, *Chemosphere.* 69 (2007) 1351–1360.
- [16] P.N. Borase, P.B. Thale, S.K. Sahoo, G.S. Shankarling, *Sens. Actuators B.* 215 (2015) 451–458.
- [17] B. Naskar, R. Modak, Y. Sikdar, D.K. Maiti, A. Bauzá, A. Frontera, S. Goswami, *Sens. Actuators B.* 239 (2017) 1194–1204.
- [18] Y. Chen, X. Wang, K. Wang, X. Zhang, *Spectrochim. Acta A.* 161 (2016) 144–149.
- [19] J.L. Pablos, S. Ibeas, A. Muñoz, F. Serna, F.C. García, J.M. García, *Reactive and Functional Polymers.* 79 (2014) 14–23.
- [20] Z. Jiang, L. Tang, F. Shao, G. Zheng, P. Lu, *Sens. Actuators B.* 134 (2008) 414–418.
- [21] J.S. Wu, W.M. Liu, X.Q. Zhuang, *Org. Lett.* 9 (2007) 33–36.
- [22] X.L. Tang, X.H. Peng, W. Dou, J. Mao, J.R. Zheng, W.W. Qin, W.S. Liu, J. Chang, X.J. Yao, *Org. Lett.* 10 (2008) 3653–3656.
- [23] L. Li, Y.Q. Dang, H.W. Li, B. Wang, Y.Q. Wu, *Tetrahedron Lett.* 51 (2010) 618–621.
- [24] K. Rurack, M. Kollmannsberger, U. Resch-Genger, J. Daub, *J. Am. Chem. Soc.*, 2000, 122, 968–969.
- [25] M. Zhang, M.X. Yu, F.Y. Li, M.W. Zhu, M.Y. Li, Y.H. Gao, L. Li, Z.Q. Liu, J.P. Zhang, D.Q. Zhang, T. Yi, C.H. Huang, *J. Am. Chem. Soc.* 129 (2007) 10322–10323.
- [26] M. Zhao, L. Ma, M. Zhang, W. Cao, L. Yang, L.J. Ma, *Spectrochim. Acta, Part A.* 116 (2013) 460–465.
- [27] H. M. Wu, P. Zhou, J. Wang, L. Zhao, C.Y. Duan, *New J. Chem.*, 33 (2009) 653–658.
- [28] Z.X. Li, L.F. Zhang, X.Y. Li, Y.K. Guo, Z.H. Ni, J.H. Chen, L.H. Wei, M.M. Yu, *Dyes and Pigments.* 94 (2012) 60–65.
- [29] M. Li, H.Y. Lu, R.L. Liu, J.D. Chen, C.F. Chen, *J. Org. Chem.* 77 (2012) 3670–3673.
- [30] E.H. Hao, T. Meng, M. Zhang, W.D. Png, Y.Y. Zhou, L.J. Jiao, *J. Phys. Chem. A* 115 (2011) 8234–8241.
- [31] D. Ray, P.K. Bharadwaj, *Inorg. Chem.* 47 (2008) 2252–2254.
- [32] J.S. Wu, W.M. Liu, X.Q. Zhuang, *Org. Lett.* 9 (2007) 33–36.

- [33] X.L. Tang, X.H. Peng, W. Dou, J. Mao, J.R. Zheng, W.W. Qin, W.S. Liu, J. Chang, X.J. Yao, *Org. Lett.* 10 (2008) 3653–3656.
- [34] L. Li, Y.Q. Dang, H.W. Li, B. Wang, Y.Q. Wu, *Tetrahedron Lett.* 51 (2010) 618–621.
- [35] J. Mao, L. Wang, W. Dou, X. Tang, Y. Yan, W. Liu, *Org. Lett.* 9 (2007) 4567–4570.
- [36] P. Saluja, H. Sharma, N. Kaur, N. Singh, D.O. Jang, *Tetrahedron.* 68 (2012) 2289–2293.
- [37] J.C. Qin, Z.Y. Yang, L. Fan, X.Y. Cheng, T.R. Li and B.D. Wang, *Anal. Methods.* 6 (2014) 7343-7348.
- [38] Y.P. Li, Q. Zhao, H.R. Yang, S. J. Liu, X. M. Liu, Y.H. Zhang, T. L. Hu, J. T. Chen, Z. Chang and X.H. Bu, *Analyst.* 138 (2013) 5486-5494.
- [39] M. Iniya, D. Jeyanthi, K. Krishnaveni, A. Mahesh, D. Chellappa, *Spectrochim. Acta A.* 120 (2014) 40-46.
- [40] W. H. Ding, W. Cao, X.J. Zheng, D. C. Fang, W. T. Wong, and L.P. Jin, *Inorg. Chem.* 52(2013) 7320-7322.
- [41] J. F. Wang, Y. Pang, *RSC Adv.* 4 (2014) 5845-5848.
- [42] a) R. Hosseinzadeh, M. Mohadjerani, M. Pooryousef, *J. Lumin.* 30 (2015) 549-555; b) R. Hosseinzadeh, M. Mohadjerani, M. Pooryousef, *Anal. Bioanal. Chem.* 408 (2016): 1901-1908. c) R. Hosseinzadeh, M. Nemati, R. Zadmand, M. Mohadjerani, *Beilstein J. Org. Chem.* 12 (2016): 1749–1757; d) R. Hosseinzadeh, M. Nemati, R. Zadmand, M. Mohadjerani, *Sens. Actuators B.* 241 (2017) 690-697.
- [43] G.B. Chalmardi, M. Tajbakhsh, A. Bekhradnia, R. Hosseinzadeh, *Inorganica Chimica Acta.* 462 (2017) 241–248.
- [44] S.N. Azizi, P. Shakeri, M.J. Chaichi, A. Bekhradnia, M. Taghavi, M. Ghaemy, *Spectrochim. Acta, Part A.* 122 (2014) 482–488.
- [45] S.N. Azizi, M.J. Chaichi, P. Shakeri, A. Bekhradnia, *J Fluoresc.* 23 (2013) 227–235.
- [46] S.N. Azizi, M.J. Chaichi, P. Shakeri, A. Bekhradnia, *J. Lumin.* 144 (2013) 34–40.
- [47] W.E. Kuhn, *Org. Synth.* (1943) 74-74.
- [48] M.Z. Kassaei, A.R. Bekhradnia, *J. Biosci. Bioeng.* 95 (2003) 526-529.
- [49] A. Bekhradnia, E. Domehri, M. Khosravi, *Spectrochim Acta Part A.* 152 (2016) 18–22.
- [50] X. Chen, T. Pradhan, F. Wang, J.S. Kim, J. Yoon, *Chem. Rev.* 112 (2011) 1910-1956.
- [51] J.C. Qin, L. Fan, Z.Y. Yang, *Sens. Actuators B Chem.* 228 (2016) 156–161.
- [52] a) D.P. Singh, R. Dwivedi, A.K. Singh, B. Koch, P. Singh, V.P. Singh, *Sens. Actuators B Chem.* 238 (2016) 128-137. b) S. Goswami, A. K. Das, A.K. Maity, A. Manna, K.S. AichMaity, P. Saha, T.K. Mandal, *Dalton Trans.* 43 (2014) 231-239. c) R. Golbedaghi, M. Rezaeivala, M. Khalili, B. Notash, J. Karimi, *Journal of Molecular Structure.* 1125 (2016) 144-148.
- [53] a) S. Arshadi, A. R. Bekhradnia, A. Ebrahimnejad, *Can. J. Chem.* 89 (2011) 403–1409. b) A. Bekhradnia, P.-O. Norrby, *Dalton Trans.* 44 (2015) 3959-3962. (c) S.Arshadi, A.R. Bekhradnia, S. Ahmadi, A.R. Karami, S. Pourbeyram, *Chin. J. Chem.* 29 (2011), 1347—1352.
- [54] M.J. Frisch, G.W. Trucks, H.B. Schlegel, G.E. Scuseria, M.A. Robb, J.R. Cheeseman, G. Scalmani, V. Barone, B. Mennucci, G.A. Petersson, H. Nakatsuji, M. Caricato, X. Li, H.P. Hratchian, A.F. Izmaylov, J. Bloino, G. Zheng, J.L. Sonnenberg, M. Hada, M. Ehara, K. Toyota, R. Fukuda, J. Hasegawa, M.I. Shida, T. Nakajima, Y. Honda, O. Kitao, H. Nakai, T. Vreven, J.A. Montgomery Jr., J.E. Peralta, F. Ogliaro, M. Bearpark, J.J. Heyd, E. Brothers, K.N. Kudin, V.N. Staroverov, R. Kobayashi, J. Normand, K. Raghavachari, A. Rendell, J.C. Burant, S.S. Iyengar, J. Tomasi, M. Cossi, N. Rega, N.J. Millam, M. Klene, J.E. Knox, J.B. Cross, V. Bakken, C. Adamo, J. Jaramillo, R. Gomperts, R.E. Stratmann, O. Yazyev, A.J. Austin, R. Cammi, C. Pomelli, J.W. Ochterski, R.L. Martin, K. Morokuma, V.G. Zakrzewski, G.A. Voth, P. Salvador, J.J. Dannenberg, S. Dapprich, A.D. Daniels, O. Farkas, J.B. Foresman, J.V. Ortiz, J. Cioslowski, D.J. Fox, Gaussian, Inc., Wallingford CT Gaussian 09, Revision A.1, Gaussian, Inc., Wallingford CT, 2009.
- [55] J. Tomasi, B. Mennucci, R. Cammi, *Chem. Rev.* 105 (2005) 2999-3094.
- [56] V.P. Singh, K. Tiwari, M. Mishra, N. Srivastava, S. Saha, *Sens. Actuators B.* 182 (2013) 546-554.
- [57] D. Karak, S. Lohar, A. Banerjee, A. Sahana, I. Hauli, S. K. Mukhopadhyay, J. S. Matalobos, D. Das, *RSC Adv.* 2 (2012) 12447-12454.
- [58] D. Karak, S. Lohar, A. Sahana, S. Guha, A. Banerjee, D. Das, *Anal. Methods,* 4 (2012) 1906-1908.
- [59] W. H. Hsieh, C. F. Wan, D. J. Liao, A. T. Wu, *Tetrahedron Lett.* 53 (2012) 5848-5851.
- [60] (a) J.S. Wu, W.M. Liu, X.Q. Zhuang, F. Wang, P.F. Wang, S.L. Tao, S.T. Lee, *Org. Lett.* 9 (2007) 33-36. (b) D. Ray, P.K. Bharadwaj, *inorg. Chem.* 47 (2008) 2252-2254. (c) H.Y. Li, S. Gao, Z. Xi, *Inorg. Chem. Commun.* 12 (2009) 300-303. (d) W. Liu, L. Xu, R. Sheng, P. Wang, H. Li, S. Wu, *Org. Lett.* 9 (2007) 3829-3832. (e) L. Li, Y.Q. Dang, H.W. Li, B. Wang, Y. Wu, *Tetrahedron Lett.* 51(2010), 618-621.

- [61] Y. P. Li, Q. Zhao, H. R. Yang, S. J. Liu, X. M. Liu, Y. H. Zhang, T. L. Hu, J. T. Chen, Z. Chang and X. H. Bu, *Analyst*. 138 (2013) 5486-5494.
- [62] J. F. Wang and Y. Pang, *RSC Adv.* 4 (2014) 5845-5848.
- [63] J.R. Lakowicz, *Principles of fluorescence spectroscopy*, springer US. (2006)
- [64] J.Y. Jung, S.J. Han, J. Chun, C. Lee, J. Yoon, *Dyes and Pigments*. 94 (2012) 423-426.
- [65] E. Özcan, S.O. Tümay, H.A. Alidağı, B. Çoşut, S. Yeşilot, *Dyes and Pigments*. 132 (2016) 230-236.
- [66] (a) S. Goswami, A.K. Das, A.K. Maity, A. Manna, K. Aich, S. Maity, P. Saha, T.K. Mandal, *Dalton Trans.* 43 (2014) 231-239.
- (b) J. Tian, X. Yan, H. Yang, F. Tian, *RSC Advances*. 129 (2015) 107012-107019.
- (c) Y. Yang, H. Xue, L. Chen, R. Sheng, X. Li, K. Li, *Chin. J. Chem.* 31 (2013) 377-380.
- [67] P. Saluja, H. Sharma, N. Kaur, N. Singh, D.O. Jang, *Tetrahedron*. 68 (2012) 2289-2293.
- [68] H. Kim, B.A. Rao, J.W. Jeong, S. Mallick, S.-M. Kang, J.S. Choi, C.S. Lee, Y.A. Son, *Sens. Actuators B.* 210 (2015) 173-182.
- [69] L. K. Kumawat, N. Mergu, M. Asif, V. K. Gupta, *Sens. Actuators B.* 231 (2016) 847-859.
- [70] Y.J. Jang, Y.H. Yeon, H.Y. Yang, J.Y. Noh, I.H. Hwang, C. Kim, *Inorg. Chem. Commun.* 33 (2013) 48-51.
- [71] A. K. Mahapatra, S. S. Ali, K. Maiti, S. K. Manna, R. Maji, S. Mondal, P. Sahoo, *RSC Adv.* 99 (2015) 81203-81211.
- [72] W. Zhu, L. Yang, M. Fang, Z. Wu, Q. Zhang, F. Yin, Q. Huang, C. Li, *J. Lumin.* 158 (2015) 38-43.
- [73] W. Wang, Z. Mao, M. Wang, L. J. Liu, D. W. Kwong, C. H. Leung, D. L. Ma, *Chem. Commun.* 52 (2016) 3611-3614.
- [74] S. Saha, P. Mahato, E. Suresh, A. Chakrabarty, M. Baidya, S. K. Ghosh, A. Das, *Inorg. Chem.* 51 (2011) 336-345.
- [75] D. Maity, T. Govindaraju, *Chem. Commun.* 48 (2012) 1039-1041.